



## COLLISION EFFICIENCIES OF ALGAE AND KAOLIN IN DEPTH FILTER: THE EFFECT OF SURFACE PROPERTIES OF PARTICLES

CHIHPIN HUANG\*<sup>Ⓒ</sup>, JILL RUHSING PAN and SHUHUI HUANG

Institute of Environmental Engineering, National Chiao Tung University, Hsinchu 30039, Taiwan, R.O.C.

(First received October 1997; accepted in revised form July 1998)

**Abstract**—Column filtration experiments with 2 mm- $\Phi$  glass beads were conducted to investigate the behavior of colloids during filtration. Algae and kaolin were used as model particles, while the chemical system was altered by changing the electrolyte concentration and pH. The collision efficiencies from the interaction between colloids and the filter medium were calculated with a semi-empirical approach of the single sphere model and clean-bed filtration theory. The experimental results indicate that ionic strength enhance the removal efficiencies for both algae and kaolin particles significantly. The removal efficiency of the filter for algae decreased with the increase in pH for up to pH 6. No significant change was observed beyond pH 6. Removal efficiencies for kaolin decreased with an increase in pH. It is concluded that collision efficiencies are sensitive to ion strength and pH. © 1999 Elsevier Science Ltd. All rights reserved

*Key words*—filtration, algae, kaolin, collision efficiency, zeta potential

### SYMBOLS

$\eta$	single-collector efficiency
$P_e$	Peclet number, defined as $P_e = 2a_c U / D_{BM}$
$N_{LO}$	London force parameter, defined as $H / 9\pi\mu a_p^2 U$
$N_R$	interception parameter, defined as $a_p / a_c$
$N_G$	gravitational parameter, defined as $2a_p^2(\rho_p - \rho)g / 9\mu U$
$A_s$	Happel's parameter, defined as $2(1 - p^5) / w$ , $p = (1 - \varepsilon)^{1/3}$ , $w = 2 - 3p + 3p^5 - 2p^6$
$D_{BM}$	Brownian diffusivity, defined as $kT / (6\pi\mu a_p)$
$a_p$	radii of suspended particles (m)
$a_c$	radii of the collectors (m)
$U$	approach velocity to a collector (m/s)
$H$	Hamaker constant (J)
$(C/C_0)_0$	clean bed removal efficiency
$\varepsilon$	porosity of the filter bed
$L$	column depth (m)

### INTRODUCTION

The filtration process is divided into two sequential steps involving transportation and attachment (O'Melia, 1985). Macroscopically, the colloidal par-

ticles are first transported from the bulk of the fluid to the vicinity of the stationary surface by physical forces, followed by attachment to the collectors through various chemical interaction at short distance (Amirtharajah and Wetstein, 1980). The theory of depth filtration has been studied in two directions (Mau, 1992): (1) a macroscopic approach called phenomenological theory, which applies mass balance to describe the filtration condition and (2) a microscopic approach, known as trajectory theory, which focuses on the properties of particle motion near a collector. The phenomenological theory of filtration has two shortcomings: the lack of generality and the failure to provide a fundamental understanding of the mechanism of deposition. Conversely, the trajectory theory examines the deposition of each particle on the collector as suspension flows through the collector. The trajectory models may be divided into two categories: one is an external flow model and the other one is an internal flow model. Both models assume particle paths far from grains following fluid streamlines. As a particle approaches a collector, the motion deviates from the streamline because of various forces acting on the particle. These forces are represented by the transportation and attachment mechanism. Our goal, through the investigation of the particle filtration in a packed column, is to calculate single-collector efficiency ( $\eta$ ) and to determine the collision (or attachment) efficiency ( $\alpha$ ) with the observed removal efficiency and the calculated value of  $\eta$ .

\*To whom all correspondence should be addressed. [Tel.: +886-3-5726463; Fax: +886-3-5725958; E-mail: cphuang@green.ev.nctu.edu.tw].

The rationale of  $\eta$  involves the physical aspect of a better understood filtration model, while  $\alpha$  accounts for the less important factors in the chemical aspect (Elimelech, 1992). Litton and Olson (1993) have successfully adopted this concept in evaluating the importance of porous medium selection and preparation method in determining attachment efficiency. In this study, the method developed by Rajagopalan and Tien (1976) was applied to obtain the single-collector collision efficiency. Green algae and kaolin were the model colloidal particles in our column filtration experiments. Our approaches first involved presenting the filtration efficiencies of particles with adjusting the pH and ionic strength of suspension and then we applied the semi-empirical model and filtration theory to estimate their collision efficiencies in the filter.

### THEORETICAL APPROACH

With the combination of trajectory and dimensional analysis, the process of filtration can be formulated. The calculation of the single-collector efficiency has been derived by Rajagopalan and Tien (1976) as follows:

$$\eta = 4A_s^{1/3} P_e^{-2/3} + 0.72A_s N_{LO}^{1.8} N_R^{15/8} + 0.0024A_s N_G^{1.2} N_R^{-0.4} \quad (1)$$

where  $P_e$  represents the role of diffusion and  $N_{LO}$  reflects van der Waals interaction.  $N_R$ , indicating the importance of interception, is the ratio of the size of suspended particle to the size of collector and  $N_G$  accounts for gravity effect. These quantities are listed in the first section.

By applying the clean-bed filtration model and a mass balance of particles over a differential packed-bed volume, the experimental collision efficiency ( $\alpha_{exp}$ ) can be related to the initial (clean-bed) removal,  $(C/C_0)_0$ , as follows (Elimelech and O'Melia, 1990):

$$\alpha_{exp} = -\ln(C/C_0)_0 \left( \frac{4a_c}{3(1-\varepsilon)L\eta_r} \right) \quad (2)$$

where  $a_c$  is the radius of the collector,  $\varepsilon$  is the porosity of the filter bed,  $L$  is the column depth and  $\eta_r$  is the single-collector efficiency. The clean bed removal efficiency,  $(C/C_0)_0$ , is the value taken at the time corresponding to a complete breakthrough curve of an inert tracer.

### MATERIALS AND METHODS

The experimental set-up consisted a stock sample tank with stirrer, pump, filter column, and fraction collector. The filter column, a 21 mm i.d.  $\times$  10 cm acrylic column with two adjustable bed supports, was packed with 2-mm glass beads. These glass beads were first cleaned by soaking in the hot 10 g/l Alconox detergent solution for at least 2 h and then rinsing a few times with de-ionized water. Thereafter, glass beads were again soaked in 5 N nitric acid for at least 12 h and then finally were rinsed with de-ionized water. All de-ionized water used for glassware washing and solution preparation was obtained from a Milli-Q system (Millipore). The porosity of the media used in this study was measured to be 0.379 by the volumetric method, and the column specifications are given in Table 1. Algae and kaolin suspensions were fed to the column by a peristaltic pump at a volumetric flow rate of 2.1 ml/min (the corresponding average residence time was 6.54 min).

The algae species, *Selenastrum capricornutum*, used in this study is one of the six freshwater algae which have been suggested by APHA et al. (1992) for the bioassay. Algae was incubated in a 50-ml nutrient medium suggested by Miller et al. (1978) for about 4 days in a shaker at 24°C. This growth medium contained six major components including 25.5 mg NaNO<sub>3</sub>, 5.7 mg MgCl<sub>2</sub> 6H<sub>2</sub>O, 4.41 mg CaCl<sub>2</sub> H<sub>2</sub>O, 14.7 mg MgSO<sub>4</sub> 7H<sub>2</sub>O, 1.04 mg K<sub>2</sub>HPO<sub>4</sub> and some trace elements (e.g. B, Mn, Zn, Co, Cu, Mo, Fe) per liter de-ionized water. About  $7.4 \times 10^6$  cells/ml of algae particles were obtained after a 4-day incubation period. 30 mg/l of kaolin suspension was prepared for each column filtration experiment.

Two approaches to measure particle size have been conducted in this study. One was measured by a particle size analyzer (PSA) with automatic image scanner (Galai Production LTD, Israel) and the other was directly observed through scanning electric microscopy (SEM) (Hitachi S-2300, Japan). The results from PSA indicated that average Feret's diameters for kaolin and algae par-

Table 1. Parameters used for filtration model calculations

Parameter	Value
Column length (m)	0.1
Column i.d. (m)	0.021
Media size ( $d_c$ ) (m)	0.002
Porosity ( $\varepsilon$ )	0.397
Kaolin diameter ( $d_p$ ) (m)	$4.3 \times 10^{-6}$
Algae diameter ( $d_p$ ) (m)	$5.0 \times 10^{-6}$
Kaolin specific gravity	2.67
Algae specific gravity	1.09
Temperature (°C)	25
Fluid viscosity, $\mu$ [(N·s)/m <sup>2</sup> ]	$8.94 \times 10^{-4}$
Fluid density (kg/m <sup>3</sup> )	997
Approach velocity, $U$ (m/s)	$1.01 \times 10^{-4}$
Gravitational acceleration, $g$ (m/s <sup>2</sup> )	9.8
Boltzmann constant (J/K)	$1.38048 \times 10^{-23}$
Hamaker constant [J ( $\times 10^{20}$ )] (estimated value)	$H_{water} = 3.7, H_{glass} = 6.5, H_{kaolin} = 10, H_{algae} = 3.0$
Hamaker constant (J) (calculated value)	$H_{k-w-g} = -7.8 \times 10^{-21}, H_{a-w-g} = 1.2 \times 10^{-21}$

ticles were  $3.9 \pm 1.71$  and  $4.2 \pm 1.33$ , respectively. Because *Selenastrum* cells are crescent-shaped, we, therefore, used the equation:  $[\text{long diameter (a)} \times \text{short diameter (b)}]^{1/3}$  to calculate the diameter equivalent to a spheric particle (d). The results from the measurement through SEM showed that kaolin had a diameter from 4 to 5  $\mu\text{m}$  and *Selenastrum* cells had lengths ranging from 6 to 8  $\mu\text{m}$  and widths from 2 to 3  $\mu\text{m}$ . The average equivalent diameters for kaolin and algae particles then can be calculated to be 4.6 and 5.0  $\mu\text{m}$ , respectively. In this study, we chose these two values from SEM measurement, not from PSA, for later calculations.

Zeta ( $\zeta$ ) potentials of algae and kaolin particles were measured with a zeta meter (System 3.0, Zeta-Meter, U.S.A.). Algae suspensions used for  $\zeta$  potential and column experiments were prepared by diluting the broth with de-ionized water. The concentration of the background electrolyte ( $\text{NaClO}_4$ ) was adjusted to give a wide range from 0.001 to 0.1 M. The pHs of the colloidal suspensions in column experiments were adjusted to 3, 5, 6, 7, 8 and 9 with 0.1 and 0.01 N  $\text{HClO}_4$  and  $\text{NaOH}$ . Prior to each experimental run, the entire system was filled with a given concentration of  $\text{NaClO}_4$  solution with the upflow mode for at least 30 min. Experiments were carried out at room temperature (23–25°C) with downward vertical flow at 2.1 ml/min (approach velocity =  $1.01 \times 10^{-4}$  m/s). The filtrate was collected by the fraction collector at a 2-min interval from 0 to 40 min. The collected filtrate of kaolin was analyzed by UV (420 nm). The quantity of algae in the filtrate was numerated by the coulter counter (Coulter electronics, U.S.A.).

## RESULTS AND DISCUSSION

### Surface properties of algae and kaolin particles

The  $\zeta$  potentials of algae and kaolin in different ionic strength as a function of pH are presented in Figs 1 and 2, respectively. It appears that the  $\zeta$

potentials of both algae and kaolin decrease with increasing  $\text{NaClO}_4$  concentrations. The increase in ionic strength enhances the electrical-double-layer compression, thereby resulting in a decrease in repulsive force and  $\zeta$  potential. When the pH is lower than 6, the  $\zeta$  potential of algae increase negatively. When the pH is higher than 6, the  $\zeta$  potential remains the same regardless of pH variation. This phenomenon can be explained by the ionization of N-functional groups on the algal surface. Protein molecules, which consist essentially of  $\alpha$ -amino acids linked by peptide ( $-\text{CONH}-$ ) linkages, are the major component of the algal membrane. The surface charge of algae originates from the ionization of N- and C-functional groups of the amino acids. All naturally occurring N-functional groups may form a stable five-member ring chelated with  $\text{Ca}^{2+}$  and  $\text{Mg}^{2+}$  provided by the nutrient, thereby resulting in the neutralization of the amino groups, and leaving the carboxyl groups as the major charged sites on the algae surface. Because of the  $\text{p}K_a$  values of carboxyl groups of amino acids, from 1.71 to 3.0 (Smith and Martell, 1976), 99% of the  $-\text{COOH}$  groups ionize to  $-\text{COO}^-$  group when  $\text{pH} = \text{p}K_a + 2$  (i.e.  $\text{pH} = 5-6$ ), and thus explains the results in Fig. 1. The  $\zeta$  potential of kaolin increases negatively with pH as indicated in Fig. 2. The surface hydrolysis of kaolin is very similar to that of the oxide surface.

### Breakthrough curves

The breakthrough curves of column filtration are presented as  $C/C_0$ ,  $C$  and  $C_0$  are the effluent and

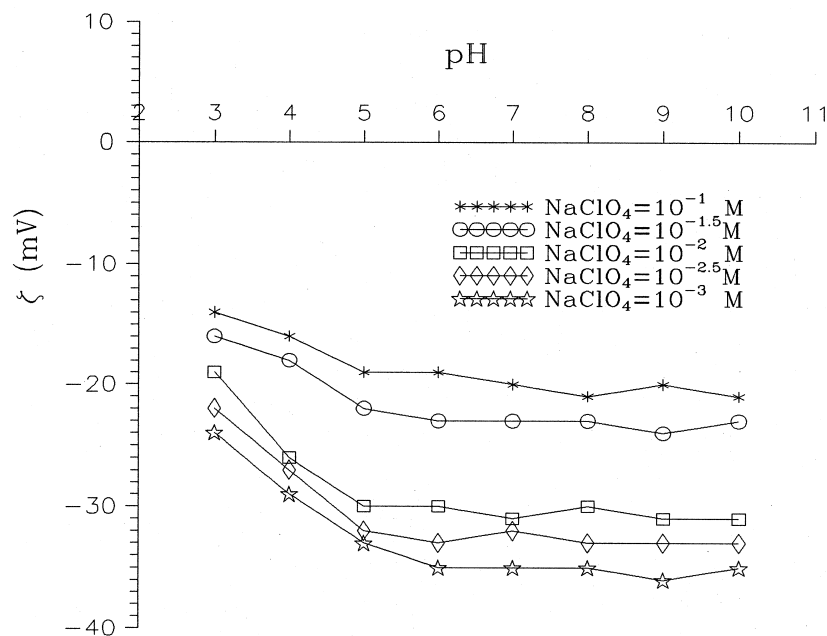


Fig. 1.  $\zeta$  potentials of algae as a function of pH with various concentrations of  $\text{NaClO}_4$ .

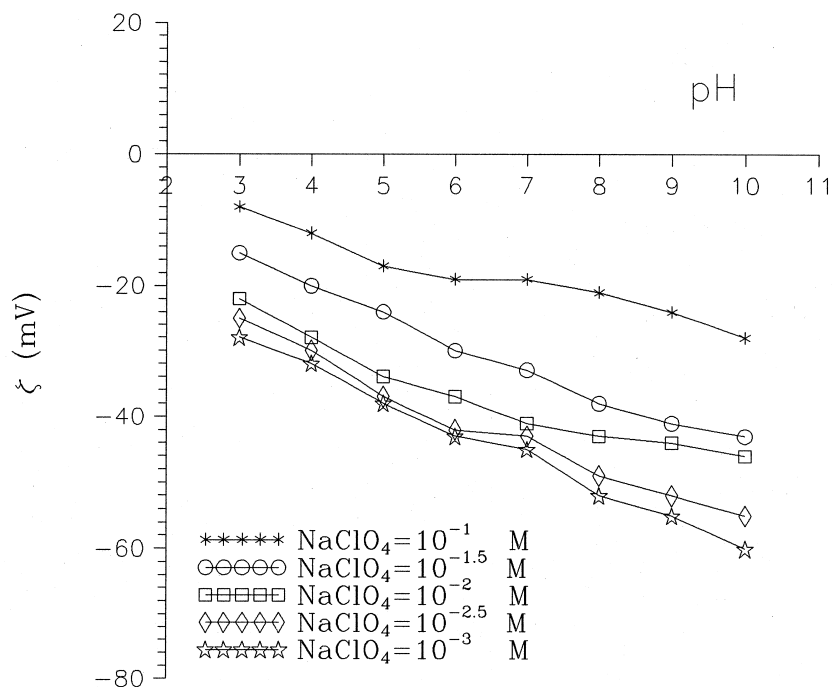


Fig. 2.  $\zeta$  potentials of kaolin as a function of pH with various concentrations of  $\text{NaClO}_4$ .

influent concentrations of particles, respectively, with respect to time. 10 min was required to complete breakthrough, which was the duration used

for the clean-bed removal of the breakthrough curve described in Fig. 3. The breakthrough curve of the inert tracer ( $\text{Cl}^-$ ) exhibits a characteristic

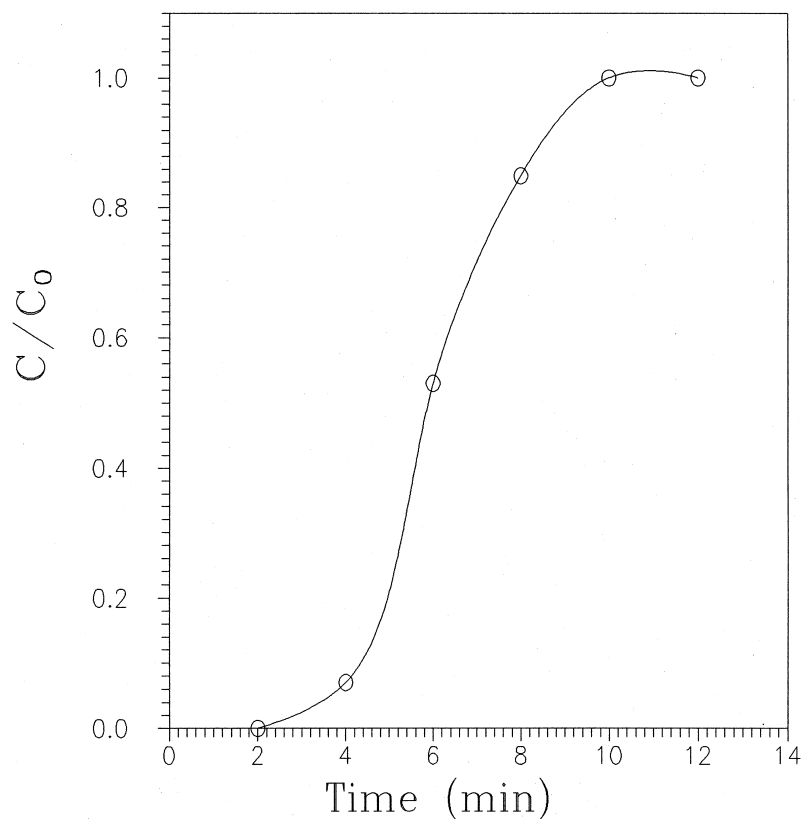


Fig. 3. Breakthrough curve of an inert tracer  $\text{Cl}^-$ . Experimental conditions were as follows: volumetric flow rate = 2.1 ml/min, bed depth = 10 cm, collector size = 2 mm.

sigmoidal shape, which is caused by the dispersion of tracer molecules in the inlet and the outlet of column.

The breakthrough curves of algae and kaolin particles at different  $\text{NaClO}_4$  concentrations are presented in Figs 4 and 5. As observed, the removal efficiencies,  $1 - C/C_0$ , of both algae and kaolin increase with  $\text{NaClO}_4$  concentrations. This finding agreed with the DLVO theory. The total interaction energy and the height of the energy barrier of the reaction decrease as the concentration of  $\text{NaClO}_4$  in the suspension increases, since the van der Waals interaction is independent of the solution chemistry. Figure 4 also indicates that the removal of algae particles is very low ( $C/C_0$  close to 1) in the dilute salt concentrations. It infers that the repulsive force between algae and the collector is very significant compared to the van der Waals force.

Column filtration experiments of kaolin and algae suspensions were also carried out in various pH in the presence of 0.01 M  $\text{NaClO}_4$  as a background electrolyte. The effects of pH on the filtration of kaolin and algae particles are illustrated in Figs 6 and 7, respectively. Figure 6 indicates that better removal efficiency of kaolin suspensions is

found at lower pH values. It can be explained by the pH effect on  $\zeta$  potentials as shown in Fig. 2. The larger removal efficiency that kaolin suspensions have therefore at lower pH values is probably due to the reduced repulsive force between particles and collectors. However, a quite different phenomenon has been found in the algae suspensions as shown in Fig. 7. At acidic condition ( $\text{pH} < 6$ ), the removal efficiencies decrease with increasing pH, with no apparent change beyond pH 6. This finding is consistent with the pH dependence of  $\zeta$  potentials as shown in Fig. 1.

#### Model parameters

Several uncertainties are involved in determining the single collector efficiency for algae and kaolin filtration. One is the average diameter of particles. When the particle size is smaller than  $1 \mu\text{m}$ , which is the size of the Brownian particle, the mechanism of the particle transport is dominated by diffusion. Therefore a decrease in the size of the Brownian particle will result in a better collector efficiency in the deep filter. As for non-Brownian particles, transport is controlled by gravity, fluid drag and interception in the deep filter. Therefore, larger

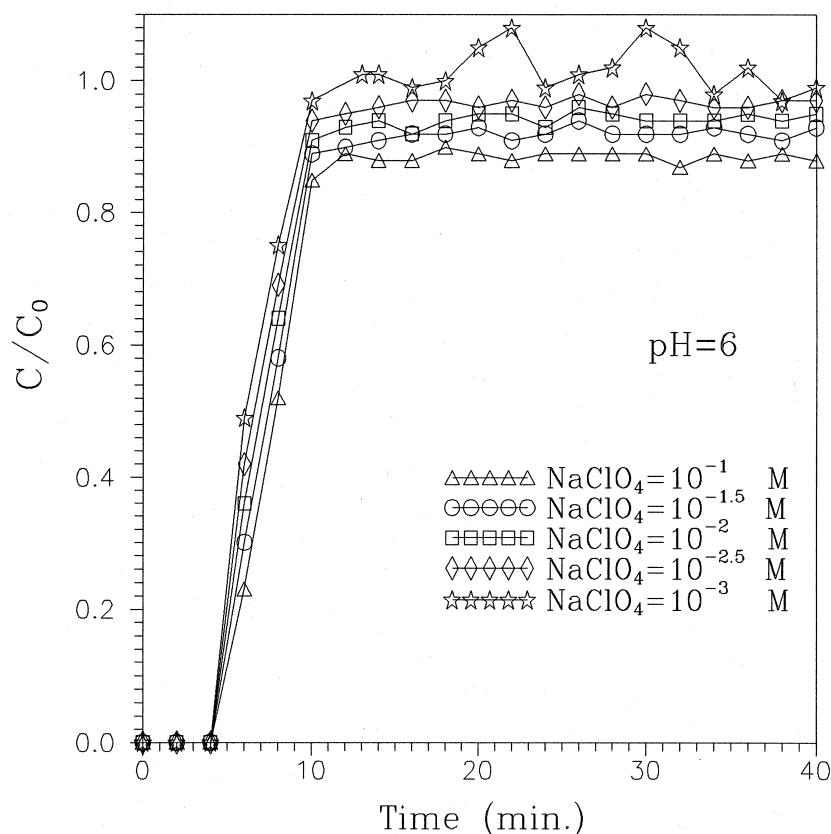


Fig. 4. Breakthrough curves of algae with various concentrations of  $\text{NaClO}_4$  at pH 6.

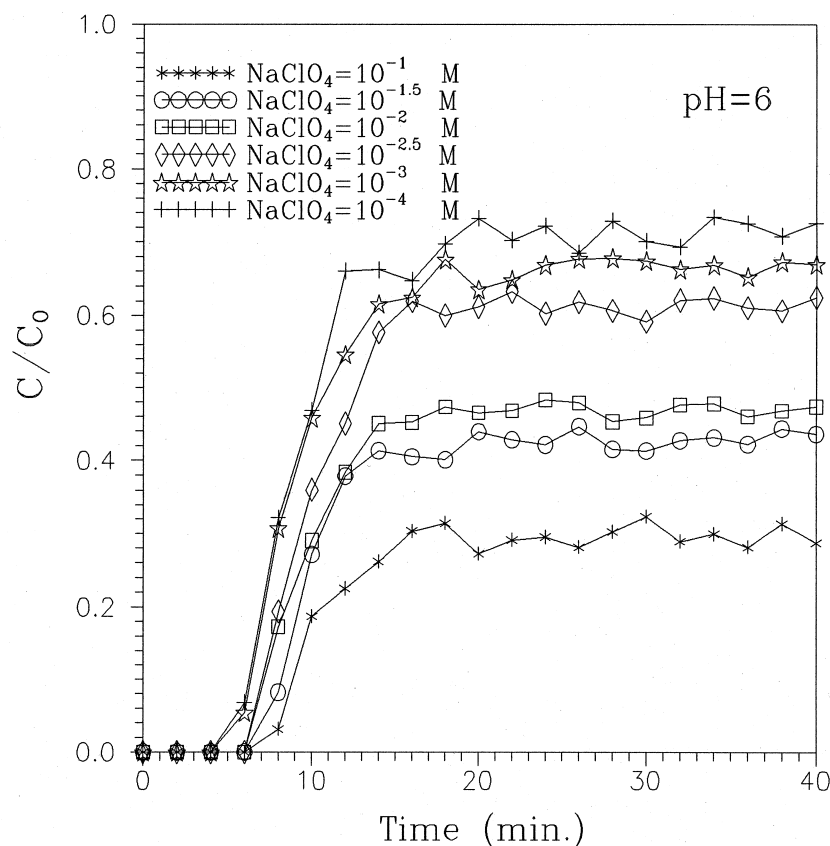


Fig. 5. Breakthrough curves of kaolin with various concentrations of  $\text{NaClO}_4$  at pH 6.

particles will result in better collector efficiency. In this study, the average diameters of algae and kaolin are measured to be 5.0 and 4.3  $\mu\text{m}$ , respectively, with a particle size analyzer as described previously.

The second uncertainty is the density of the particle ( $\rho_p$ ). The specific gravity of kaolin was determined as 2.67 from the gravity test. On the other hand, it is difficult to determine the density of algae due to its natural buoyancy in the suspension. Little information is available on the range of buoyant densities of algae in aquatic systems. However, it may be assumed that most algae in water have near neutral buoyancy, judged from their slow settling velocities. Algae, being a biological entity, contain mostly water. When suspended in solution, they are capable of adjusting their water content in order to float in the medium freely. As a result, they don't have an exact density. This has been mentioned by Ronald (1991) in his study of modeling the movement of bacteria through a sandy aquifer using colloid filtration theory. When clean-bed filtration theory was applied to bacterial deposition in porous media, Martin *et al.* (1992) mentioned the same difficulty and adopted 1.04, 1.10 and 1.13 as

the density of bacteria. Since algae behave the same as the bacteria in water, it is reasonable to assume that they have similar densities, which is approximately 1. In the calculation of single filter collection efficiency, we have used different densities, namely 1.05, 1.07 and 1.09, to study their effect on collision attachment.

The last uncertainty is the value of Hamaker constant. Other appropriate values for the calculation of collision efficiency were adopted from the related work (Hough and White, 1980). The values of particle-water-collector have been calculated by using the Hamaker approach as listed in Table 1 previously.

#### Experimental collision efficiencies

In theory, the collision efficiency approaches unit when colloidal interactions are dominated by deposition. If not, their collision efficiencies would drop. In this study, experimental collision efficiencies (denoted as  $\alpha_{\text{exp}}$ ) can be calculated from the results of column filtration experiments. The stability curves, the logarithm of  $\alpha_{\text{exp}}$  vs the logarithm of electrolyte concentration, of kaolin and algae filtration are presented in Figs 8 and 9. A gradual

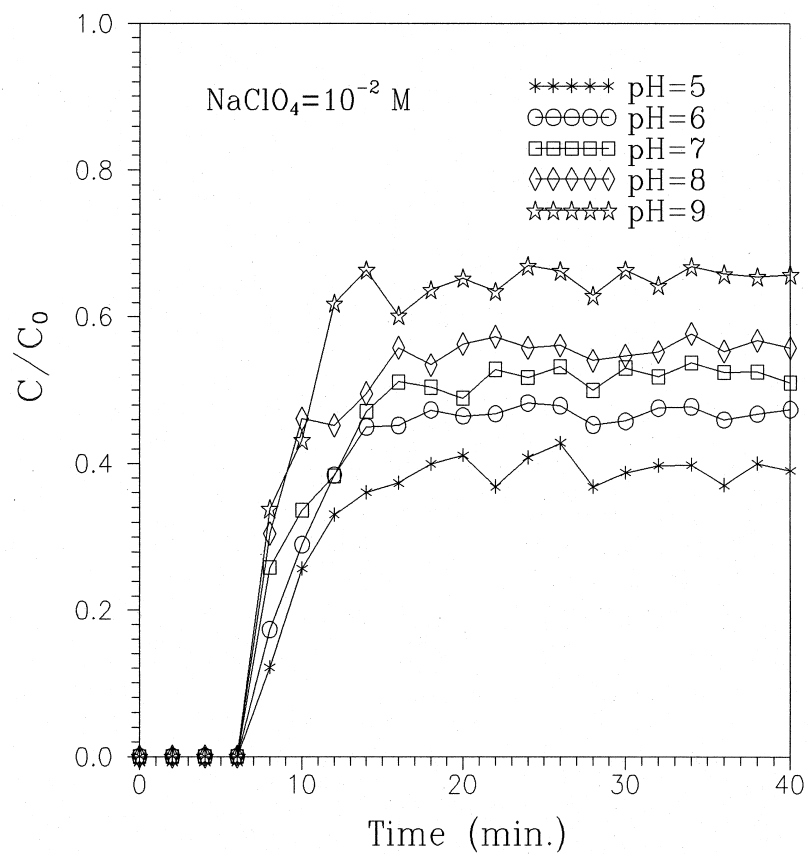


Fig. 6. Breakthrough curves of kaolin with various pH in the presence of  $0.01 \text{ M NaClO}_4$ .

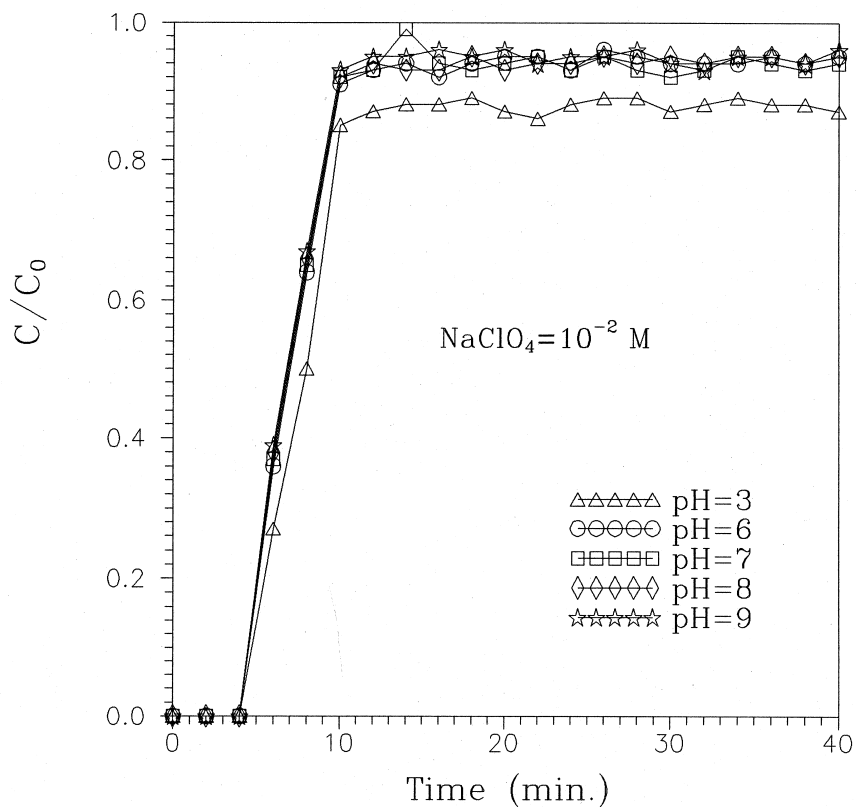


Fig. 7. Breakthrough curves of algae with various pH in the presence of  $0.01 \text{ M NaClO}_4$ .

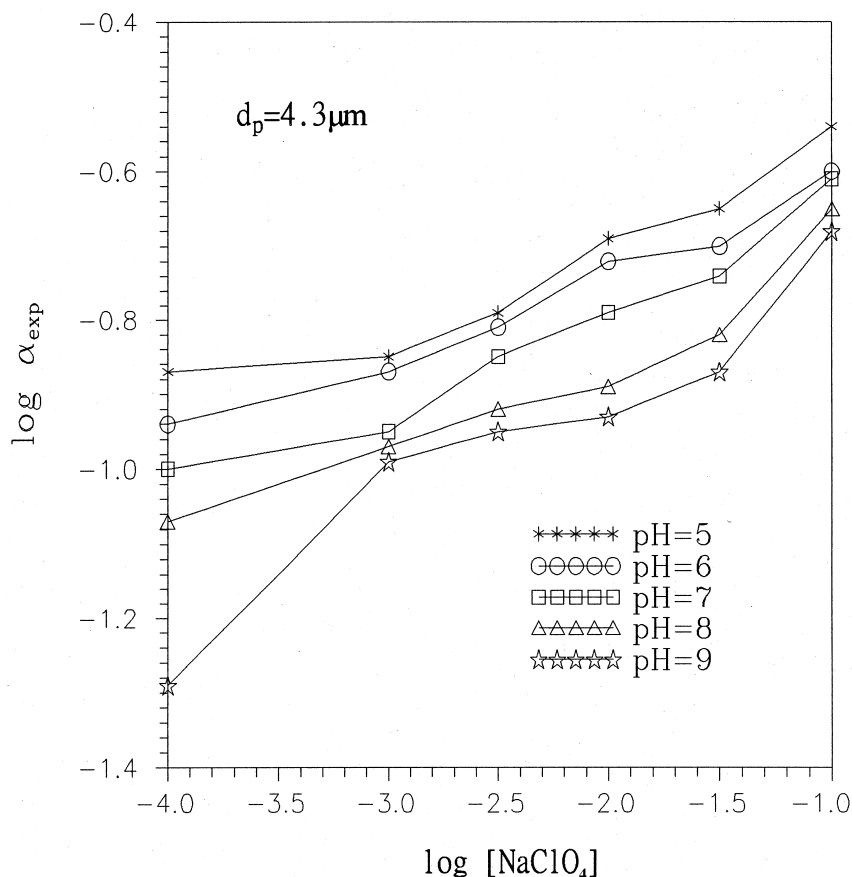


Fig. 8. Experimental stability curves of kaolin with various pH. The logarithm  $\alpha_{\text{exp}}$  is plotted as a function of the logarithm of molar  $\text{NaClO}_4$  concentrations.

increase in the collision efficiency with increasing  $\text{NaClO}_4$  concentration is observed. As the electrolyte concentration increases, the diffuse layer is compressed and therefore more colloidal particles complete the attachment process successfully. Figure 8 also points out that at the same electrolyte concentration, smaller collision efficiencies occur at kaolin suspensions of higher pH. Surface charges of kaolin particles in the water develop as a result of chemisorption of water splitting into  $\text{H}^+$  and  $\text{OH}^-$  during adsorption to form a hydroxylated surface. At higher pH,  $\text{OH}^-$  ions are adsorbed in excess onto the hydroxylated surface, thereby resulting in more negative charges on the kaolin surface. This situation of more negative charges, therefore, causes higher energy barrier and smaller collision efficiency between two particles or the particle and collector.

Figure 9 shows the experimental stability curves of algae at various pHs. It is observed that, in the pH ranging from 3 to 9, the result is similar to that of kaolin filtration, where the  $\alpha_{\text{exp}}$  value increases with electrolyte concentrations. For algae filtrations at the same electrolyte concentration, the  $\alpha_{\text{exp}}$  value

at pH 3 is larger than that at a pH above 6, with no significant change beyond pH 6. This phenomenon can be described by the variation of  $\zeta$  potentials with the pH. This is the major reason why the interaction energy between the algae and the collector is almost independent of pH, which results in a similar  $\alpha_{\text{exp}}$  value.

#### SUMMARY

A semi-empirical approach for predicting collision efficiencies of algae and kaolin particles for the colloid deposition in porous media is presented. The chemical system of suspensions was changed by adjusting the electrolyte concentrations and pH. The results reveal that the experimental collision efficiencies of both algae and kaolin particles appear to be proportional to the electrolyte concentrations as well as inversely proportional to the  $\zeta$  potentials of the particles. Kaolin filtration with higher operating-pH results in larger experimental collision efficiency. However, the experimental collision efficiencies for algae filtration decrease with an increase



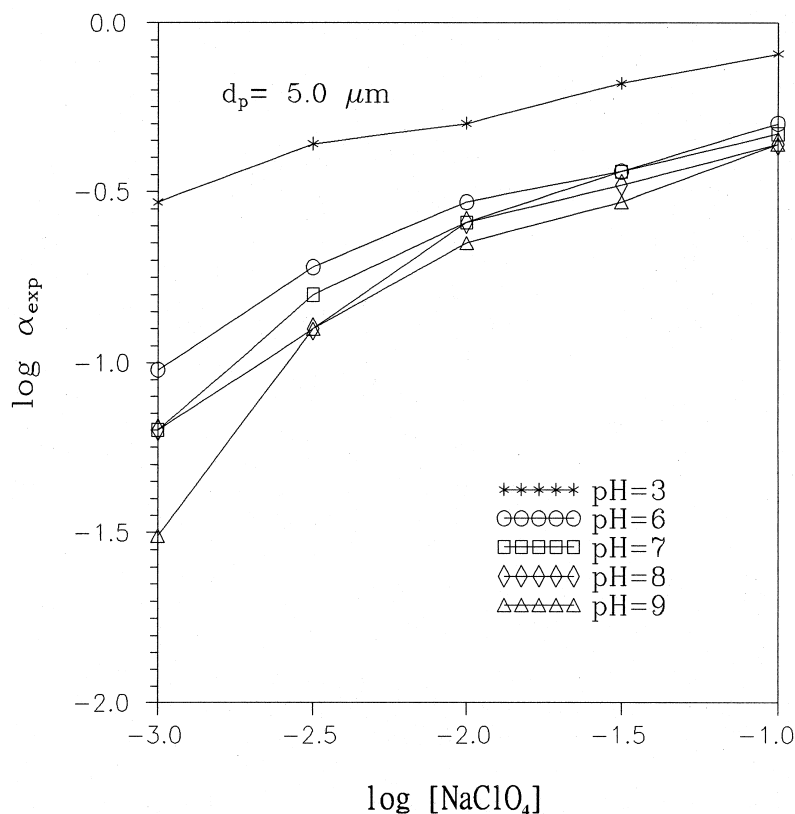


Fig. 9. Experimental stability curves of algae with various pH. The logarithm  $\alpha_{\text{exp}}$  is plotted as a function of the logarithm of molar  $\text{NaClO}_4$  concentrations.

in pH up to pH 6 and no significant change beyond pH 6.

*Acknowledgements*—The authors wish to express their gratitude for the technical assistant given by Professor C. Y. Chen and his research group in our institute. We also wish to mention our sincere gratitude to Union Chemical Laboratory, ITRI for the assistance in particle size analysis.

#### REFERENCES

- APHA, AWWA and WEF (1992) *Standard Methods for the Examination of Water and Wastewater*, 18th edn.
- Amirtharajah A. and Wetstein D. P. (1980) Initial degradation of effluent quality during filtration. *J. AWWA* **72**, 518–524.
- Elimelech M. and O'Melia C. R. (1990) Kinetics of deposition of colloidal particles in porous media. *Environ. Sci. Technol.* **24**, 1528–1536.
- Elimelech M. (1992) Predicting collision efficiencies of colloidal particles in porous media. *Water Res.* **26**, 1–8.
- Hough D. B. and White L. R. (1980) The calculation of Hamaker constants from Lifshitz theory with applications to wetting phenomena. *Adv. Colloid Interface Sci.* **14**, 3–41.
- Litton G. M. and Olson T. M. (1993) Colloid deposition rates on silica bed media and artifacts related to collector surface preparation methods. *Environ. Sci. Technol.* **27**, 185–193.
- Martin R. E., Edward J. B. and Linda M. H. (1992) Application of clean-bed filtration theory to bacterial deposition in porous media. *Environ. Sci. Technol.* **26**, 1053–1058.
- Mau R. E. (1992) Particle transport in flow through porous media: Advection, longitudinal dispersion and filtration. Ph.D. Dissertation, California Institute of Technology.
- Miller W. E., Green J. C. and Shiroyama T. (1978) *The Selenastrum capricornutum printz algal assay bottle test. Experimental design, application, and data interpretation protocol*. EPA-600/9-78-018.
- O'Melia C. R. (1985) Particles, pretreatment and performance in water filtration. *J. Environ. Eng.* **111**, 874–890.
- Rajagopalan R. and Tien C. (1976) Trajectory analysis of deep-bed filtration with the sphere-in-cell porous media model. *AIChE J.* **22**, 523–533.
- Ronald W. H. (1991) Use colloid filtration theory in modeling movement of bacteria through a contaminated sandy aquifer. *Environ. Sci. Technol.* **25**, 178–185.
- Smith R. M. and Martell A. E. (1976) *Critical Stability Constants*. Plenum Press, New York.
- Yao K. M., Mohammad T. H. and O'Melia C. R. (1971) Water and waste water filtration: concepts and applications. *Environ. Sci. Technol.* **5**, 1105–1112.